HIGHLY EFFICIENT, HIGH-ENERGY THz PULSES FROM CRYO-COOLED LITHIUM NIOBATE FOR ACCELERATOR AND FEL APPLICATIONS*

Kyung-Han Hong[#,1] Wenqian Ronny Huang,[1] Ravi Koustuban,[1] Shu-Wei Huang,[1] Eduardo Granados,[1] Luis E. Zapata,[1] and Franz X. Kärtner[1,2,3]

[1]Department of Electrical Engineering and Computer Science and Research Laboratory of Electronics, Massachusetts Institute of Technology, 77 Massachusetts Avenue, Cambridge, MA, 02139, USA

[2]Center for Free-Electron Laser Science, DESY, Notkestraße 85, D-22607 Hamburg, Germany

[3]Department of Physics, University of Hamburg, Notkestraße 85, D-22607 Hamburg, Germany

Abstract

Intense, ultrafast terahertz (THz) fields are of great interest for electron acceleration, beam manipulation and measurement, and pump-probe experiments with coherent soft/hard x-ray sources based on free electron lasers (FELs) or inverse Compton scattering sources. Acceleration at THz frequencies has an advantage over RF in terms of accessing high electric-field gradients (>100 MV/cm), while the beam delivery can be treated quasi-optically. In this paper, we present highly efficient, single-cycle, 0.45-THz pulse generation by optical rectification of 1.03-um pulses in cryogenically cooled lithium niobate (LN). Using a near-optimal duration of 680 fs and a pump energy of 1.2 mJ, we report conversion efficiencies above 3%, >10 times higher than previous report (0.24%). Cryogenic cooling of LN significantly reduces the THz absorption, which will enable the scaling of THz pulse energies to the mJ. As a preliminary experiment, we demonstrate low-energy electron acceleration or streaking by THz pulses.

INTRODUCTION

The intense and ultrafast THz fields have many interesting applications, such as THz time-domain spectroscopy, the study of carrier dynamics in semiconductors, electric field gating of interlayer charge transport in superconductors, or THz-assisted attosecond pulse generation [1-3]. More recently, high peak power THz sources have been proposed for acceleration, undulation, deflection and spatiotemporal arbitrary manipulation of charged particles, enabling compact linear accelerators for FEL facilities and inverse Compton scattering X-ray sources. These applications benefit from the scaling the energy and peak power of the THz pulses.

Optical rectification (OR) is one of the common methods for optically pumped THz generation together with difference frequency generation (DFG). In contrast to DFG, OR has been widely used to generate pulses at low THz frequencies [4]. Since the nonlinear process can be cascaded, over 100% of photon conversion efficiency has been demonstrated [5]. Compared to ZnTe, one of the common nonlinear materials used for OR, LN has multiple advantages such as large d_{eff}, high damage threshold, low THz absorption, and large bandgap, but it requires tilted pulse front pumping techniques to achieve phase matching between the IR pump and the THz wave [6]. The highest THz pulse energy that has been reported is still only 0.24%, achieved by pumping a room-temperature LN crystal with 100 mJ, 1.2 ps pulses [7].

Recent theoretical studies have shown that OR in LN can be further improved in terms of efficiency by optimizing the pump pulse duration [8], lowering the distortion produced by the imaging techniques, and reducing the photo-refractive losses in the LN crystal by cooling it down to cryogenic temperatures [9]. The optimum pump pulse duration is found to be ~500 fs because it maximizes the effective length of the nonlinear interaction for THz generation [7]. In addition, maintaining a moderate pumping fluence ensures no saturation of the THz generation process due to three-photon absorption. The maximum efficiency predicted at room temperature is ~2%. Stoichiometric lithium niobate (sLN) is more beneficial for a high efficiency than congruent lithium niobate (cLN), but growing sLN to a large size is limited. In this paper, we demonstrate an efficient THz generation in a cryogenically cooled cLN using a near optimal pump pulse duration of 680 fs.

EXPERIMENTAL SETUP AND RESULTS

The pump laser for OR is a diode-pumped sub-ps Yb:KYW chirped pulse amplification system (s-Pulse, Amplitude Systemes) at 1-kHz repetition rate. The pulses have a center wavelength at 1029 nm with 2.6 nm of spectral bandwidth. The regenerative amplifier was seeded by a mode-locked Yb-doped fiber oscillator [10] followed by a fiber stretcher and pre-amplifier. After the further stretching in a grating stretcher and the regenerative amplification to 2 mJ, the pulses were compressed to 680 fs using a grating compressor. The maximum available energy was 1.2 mJ for the experiments.

*Work supported by DARPA AXiS program under contract number N66001-1-11-4192.
#kyunghan@mit.edu

Copyright © 2013 CC-BY-3.0 and by the respective authors

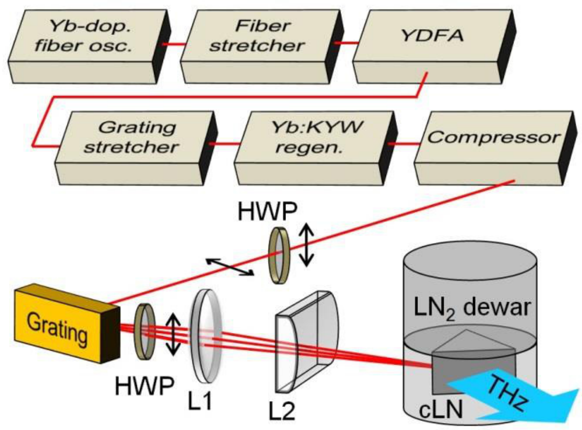

Figure 1: Experimental setup for THz generation. L1, bestform lens (f = 20 cm); L2, cylindrical lens (f = 15 cm); HWP, half wave plate.

Figure 1 illustrated the laser system and the pulse front tilting scheme using a 1500 lines/mm grating and an imaging lens with a demagnification factor of 1.54. An MgO-doped cLN prism (6.0%, z-cut, cut into an isosceles triangle with an apex angle of 56 degrees) was used for OR. The 1029-nm beam experiences total internal reflection inside the cLN, so only the input and output faces of the crystal are AR coated, whereas the third face remained uncoated. The polarization of the diffracted beam was adjusted to vertical polarization, parallel to the optic axis of the LN crystal. We utilized a cylindrical lens to obtain the pump spot size ($1/e^2$) of 3.0 mm in the horizontal and 3.0 mm in the vertical direction, achieving an optimum fluence of 17 mJ/cm^2. The crystal is indium soldered to a nickel plate that matches the thermal expansion coefficient of lithium niobate from room temperature to cryogenic temperatures to ensure no deformations and good thermal contact. The nickel plate is mounted in a cryogenic Dewar with controlled temperature. A calibrated pyroelectric detector (Microtech Instruments) was used for the THz signal measurement, while the repetition rate of the pump laser was decreased to 10 Hz to avoid saturation in the slow detector. The THz pulse energy was then measured from the voltage modulation observed with a scope.

Figure 2 depicts the THz energy as a function of the pump energy at room temperature for both sLN and cLN crystals. The THz energy increases with a power dependence of 1.80 for cLN and 1.97 for sLN without any sign of roll-off from free-carrier absorption. The maximum THz energy achieved with the sLN crystal was 21.8 µJ at 1.28 mJ of pump energy, corresponding to an efficiency of 1.7% [11]. Likewise, the maximum achieved THz energy in the cLN crystal was 13.7 µJ at 1.18 mJ of pump energy, corresponding to an efficiency of 1.16%. The conversion efficiency in sLN is greater than that in cLN by a factor of 1.47; this is expected with the ~20% increase in d_{eff} (of sLN over cLN) [12] since the efficiency is proportional to the square of d_{eff}. The experimental results of efficiency show good agreement with simulations based on the 1-D models described in [11] for the previously described experimental parameters. A d_{eff}=168 pm/V and effective interaction length of 4 mm was assumed. Since the precise dispersion in the frequency range of 0 to 0.9 THz was not known, a constant absorption coefficient of 5 cm^{-1} was assumed as an adjustable parameter. After accounting for a THz reflection of ~44% at the air-crystal interface, the calculated efficiency is 1.33% for cLN which closely matches the experimental result of 1.15%. Note that the use of adjustable parameters can be justified since the THz waveform, spectrum and efficiency calculations, all triangulate with the same parameters.

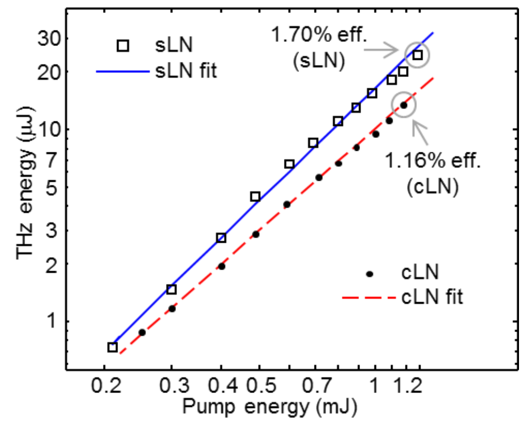

Figure 2: Pump energy sweep of THz generated from room temperature sLN and cLN. The sLN fit shows a 1.97 power dependence and the cLN fit shows a 1.80 power dependence.

Temporal characterization of the THz pulse generated from sLN at room temperature was performed by electro-optic (EO) sampling. The results for cLN are expected to be qualitatively similar. Figure 3a depicts the measured single-cycle THz waveform with a cycle period of ~2.2 ps. The theoretical calculation of the temporal electric field waveform based on the 1-D model [11] is overlaid with the experimental measurement in Fig. 3a and resembles the basic feature of the experimental result. The temporal wave form is sensitive to the tilt angle of the pulse front, the input amplitude, as well as phase spectrum of the IR pulse which can explain the discrepancy between theory and experiment. The corresponding experimental and calculated spectra are presented in Fig. 5b. It is seen that the THz pulse has a center frequency of 0.45 THz and a full-width-half-maximum (FWHM) bandwidth of 0.4 THz with a tail extending beyond 1 THz. The echo pulse at ~3.5 ps is a common artifact caused by multiple reflections of the IR probe pulses off the EO crystal and can be disregarded. Due to the echo pulse, a time window was applied prior to the Fourier transform; therefore, the typical absorption lines of water are not observed because of the limited frequency resolution. The temporal shape of the THz pulses from cryogenic LN is expected to be

Copyright © 2013 CC-BY-3.0 and by the respective authors

ISBN 978-3-95450-126-7

similar to that at room temperature except for a slightly shifted spectrum towards high frequency due to reduced losses.

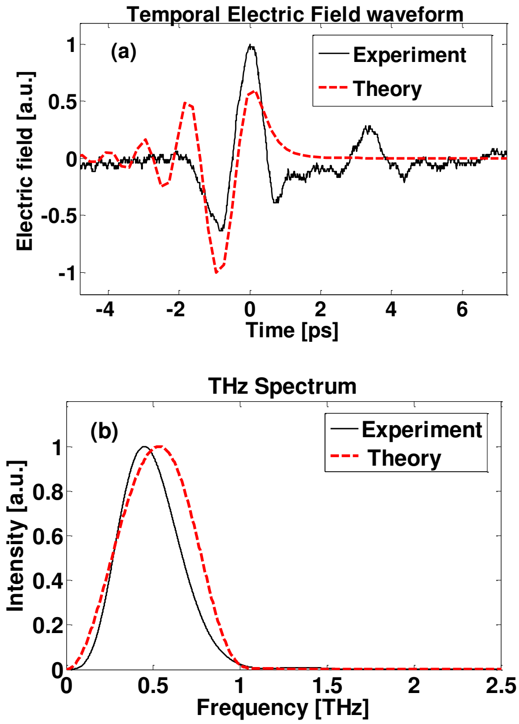

Figure 3: (a) Electric field of THz pulse as a function of time obtained by EO sampling. (b) Power spectrum of THz pulse.

To further enhance the efficiency, we lowered the absorption of LN at THz frequencies by cooling it to cryogenic temperatures. The temperature dependence of the THz power at the pump energy of 1.2 mJ is shown in Fig. 4. The THz power increases monotonically as the temperature decreases to ~150 K, below which we observe saturation of the conversion efficiency due to the slight change of phase matching condition. We obtained a maximum enhancement of 3.3, corresponding to an estimated conversion efficiency of record-high 3.8% [13].

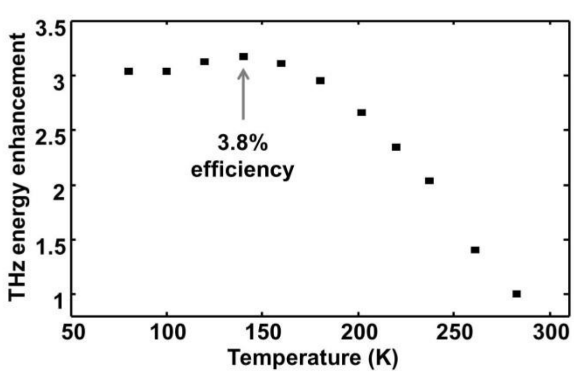

Figure 4: Efficiency enhancement versus temperature at pump energy of 1.2 mJ from cLN.

For a proof-of-principle experiment of free-space THz electron acceleration, we have implemented a THz streaking setup of photo-emitted electrons in a vacuum chamber. The sub-ps 1-μm pulse mixed with its second harmonic is used for triggering photo-emission from a copper photo-cathode. A 2-μJ THz pulse is spatially overlapped with the photo-emission area on the copper surface with an oblique angle to steer the emitted electrons towards an anode. The time delay between the THz pulse and the photo-cathode laser pulse is scanned for the investigation of the effect of THz pulses on the emitted charge, which is measured by an anode current. Dependence of the anode bias on the charge gives an estimate of the emitted electron energy. The preliminary result is shown in Fig. 5. There is a clear indication of electron acceleration up to ~40 eV when the THz pulse exists at the time delay of ~0-3 ps. The nonzero electron charge is observed even with a bias of -40 V, which has been overcome by the THz field. We have made sure that the electron charge is negligible without the THz field.

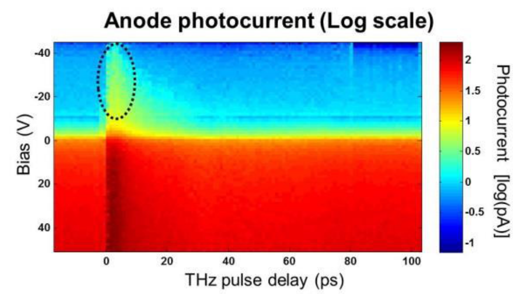

Figure 5: Photocurrent with respect to the delay between the photo-cathode laser pulse and the THz pulse at different anode biases. The region with dotted circle indicates the THz acceleration of electrons up to ~40 eV.

By further increasing THz fields using higher-energy laser pulses and employing waveguide geometry with radially polarization, we even expect to scale the electron energy to MeV range, which will be a significant step towards a compact THz-based electron accelerator.

ACKNOWLEDGMENT

The authors like to thank Dr. Alan Lee, Dr. Daniel Miller, and Hung-Wen Chen for their technical contribution.

REFERENCES

[1] J. Hebling, K.-L. Yeh, M. C. Hoffmann, and K. A. Nelson, IEEE J. Sel. Top. Quantum Electron. **14**, 345–353 (2008).
[2] H. Hirori, M. Nagai, and K. Tanaka, Phys. Rev. B **81**, 081305 (2010).
[3] A. Dienst, M. C. Hoffmann, D. Fausti, J. C. Petersen, S. Pyon, T. Takayama, H. Takagi, and A. Cavalleri, Nat. Photon. **5**, 485 (2011).

Copyright © 2013 CC-BY-3.0 and by the respective authors

ISBN 978-3-95450-126-7

[4] M. C. Hoffmann, and J. A. Fulop, J. Phys. D: Appl. Phys. **44**, 083001 (2011).
[5] K. Vodopyanov, Opt. Express **14**, 2263-2276 (2006).
[6] J. Hebling, K. Yeh, M. Hoffmann, B. Bartal, and K. Nelson, J. Opt. Soc. Am. B **25**, B6-B19 (2008).
[7] J. A. Fulop, L. Palfalvi, S. Klingebiel, G. Almasi, F. Krausz, S. Karsch, and J. Hebling, Opt. Lett. **37**, 557-559 (2012).
[8] J. A. Fulop, L. Palfalvi, M. C. Hoffmann, and J. Hebling, Opt. Express **19**, 15090-15097 (2011).
[9] L. Palfalvi, J. Hebling, J. Kuhl, A. Peter, and K. Polgar, J. Appl. Phys. **97**, 123505 (2005).
[10] K. H. Hong, A. Siddiqui, J. Moses, J. Gopinath, J. Hybl, F. O. Ilday, T.Y. Fan and F. X. Kartner, Optics Letters **33**, 2473-2475 (2008).
[11] J. A. Fulup, L. Palfalvi, G. Almasi, and J. Hebling, Opt. Express **18**(12), 12311–12327 (2010).
[12] T. Fujiwara, M. Takahashi, M. Ohama, A. J. Ikushima, Y. Furukawa, K. Kitamura, Electronics Letters **35**, 499–501 (1999).
[13] S.-W. Huang, E. Granados, W. R. Huang, K.-H. Hong, L. E. Zapata, and F. X. Kartner, Opt. Lett. **38**, 796-798 (2013).

ISBN 978-3-95450-126-7

Copyright © 2013 CC-BY-3.0 and by the respective authors